Available online at www.sciencedirect.com
SCIENCE DIRECT®
C. R. Mecanique 333 (2005) 103–110
COMPTES RENDUS MECANIQUE
http://france.elsevier.com/direct/CRAS2B/

High-Order Methods for the Numerical Simulation of Vortical and Turbulent Flows

Adaptive mesh strategy applied to turbulent flows

Alexander Hay, Michel Visonneau

Division modélisation numérique, laboratoire de mécanique des fluides CNRS UMR 6598, École centrale de Nantes, B.P. 92101, rue de la Noë, 44321 Nantes, France

Available online 28 December 2004

Abstract

An adaptive mesh procedure controlled by an error estimate for the Navier–Stokes equations is developed. The mesh can be refined but also coarsened by the mean of an agglomeration algorithm. The error estimation is based on an equation for the discretization error with a source term approximated by the use of a higher order discretized operator. The whole procedure is applied to a turbulent flow around a square-cross section cylinder. The efficiency of the method, evaluated in terms of CPU time and number of cells, shows interesting gains compared to single mesh computations. ***To cite this article: A. Hay, M. Visonneau, C. R. Mecanique 333 (2005).***

Résumé

Adaptation de maillage appliqué aux écoulements turbulents. Une procédure d'adaptation de maillage guidée par un estimateur d'erreur pour les équations de Navier–Stokes est développée. L'outil permet de raffiner le maillage et de le déraffiner par un algorithme d'agglomération de cellules. L'estimateur d'erreur est basée sur la résolution d'une équation pour l'erreur de discrétisation dont le terme source est approché en utilisant un schéma de discrétisation d'ordre élevé. La méthode est appliquée à un écoulement turbulent autour d'un cylindre de section carrée. On quantifie les gains obtenus par l'utilisation de la procédure adaptative en terme de temps et de nombre de points de calcul. ***Pour citer cet article : A. Hay, M. Visonneau, C. R. Mecanique 333 (2005).***

Keywords: Computational fluid mechanics; Finite-volume; H-Refinement; Error estimation; Turbulent Flow

Mots-clés : Mécanique des fluides numérique ; Volumes finis ; Maillage adaptatif ; Estimation d'erreur ; Ecoulement turbulent

Version française abrégée

Les techniques de maillage adaptatif ont pour objectif d'obtenir une solution numérique de précision prédéterminée pour un coût de calcul minimum en adaptant le maillage au problème considéré.

E-mail addresses: alexander.hay@ec-nantes.fr (A. Hay), michel.visonneau@ec-nantes.fr (M. Visonneau).

1631-0721/$ – see front matter
doi:10.1016/j.crme.2004.09.014

Les régions du maillage à modifier doivent être sélectionnées avec soin pour que le processus d'adaptation soit efficace. Ainsi, il est nécessaire d'estimer avec précision l'erreur de discrétisation attachée à la solution numérique sur un maillage donné pour être en mesure de la réduire en effectuant la sélection de manière fine. Pour réaliser cette estimation pour des méthodes numériques de type volumes finis, on forme une équation de transport pour l'erreur. Celle-ci présente un terme source dont on va réaliser une approximation par l'utilisation d'un schéma discret d'ordre élevé. Une description plus détaillée de cette méthode et de son utilisation est présentée dans [9].

La procédure adaptative guidée par le terme source de l'erreur permet de réduire l'erreur de discrétisation en raffinant le maillage. Le schéma de la procédure est illustré sur la Fig. 1. Le maillage peut également être déraffiné par le biais d'un algorithme d'agglomération de cellules aboutissant à des volumes de contrôle de forme quelconque (Fig. 2).

L'ensemble de l'outil d'adaptation est finalement appliqué à un écoulement turbulent ($Re = 22\,000$) autour d'un cylindre de section carrée au voisinage d'une plaque plane comme illustré sur la Fig. 3. De manière à évaluer la qualité de la solution sur le maillage adapté, des calculs sur des grilles uniformes de finesse croissante ont été effectués (Tableau 1). On peut observer sur les Figs. 7 et 8 que la solution adaptée est proche de celle de la grille fine uniforme 5. Le Tableau 1 indique que la grille adaptée comporte près de quatre fois moins de points que la grille 5 et son coût de calcul est plus de dix fois moins élevé pour obtenir une solution numérique de qualité équivalente.

1. Introduction

The goal of CFD research is to find solutions free from numerical error or at least of a desired prescribed accuracy for the lowest computational and human costs. Adaptive h-refinement techniques have been designed for reaching such a solution by dynamically refining and coarsening meshes until the error is under a prescribed value. The number of computational points is thus adapted to the asked accuracy and human effort is limited as the procedure is designed to be automatic.

The error estimate, designed in the framework of finite-volume methods, is based on an equation for the error which allows to take into account the known transport properties of the error. The equation presents a source term which is approximated by the difference between the discretized operator considered in the flow solver and a higher order operator.

This a posteriori error estimate applied to the velocity component and to the turbulent kinetic energy is used for guiding an adaptive mesh refinement/unrefinement included in a flow solver that can deal with discretization elements of arbitrary topology.

The whole procedure is applied to a complex turbulent flow around a square-cross section cylinder mounted close to a flat plate at $Re = 22\,000$ in order to evaluate the gains made by the use of an adaptive mesh strategy compared to single mesh computation.

2. Flow solver

The ISIS flow solver, developed in our laboratory, uses the incompressible Reynolds-Averaged Navier–Stokes equations. The solver is based on the finite-volume method to build the spatial discretization of the transport equations on unstructured grids. The face-based method is generalized to unstructured meshes composed of arbitrary volume shapes (they are bounded by an arbitrary number of constitutive faces). The velocity field is obtained from the momentum conservation equation and the pressure field is extracted from the mass conservation constraint transformed in a pressure equation. The whole discretization is fully implicit in space and time and is formally second order accurate. Several near-wall low-Reynolds number turbulence models, ranging from one-equation Spalart–Allmaras model [1], two-equation k–ω closures [2], to a full Reynolds stress transport R_{ij}–ω [3] model are implemented in the code.

3. A posteriori error estimation

The error considered here is often called discretization error. It involves the discretization of the equations which are to be solved as well as the discretization of the geometry and the boundary conditions which create an error due to incomplete grid convergence and imperfect grid generation (grid aspect ratio, skewness, non orthogonality). A posteriori error estimation is considered since a priori estimation is not possible for nontrivial problems [4]. Little work has been done on such techniques in the framework of finite-volume methods. Much of the methods are based on the use of the information on the derivatives of the variables treated. Furthermore, the transport of the error over the computational domain is not taken into account as only local information is considered. The present method is based on an equation for the discretization error in order to take into account the known transport properties of this quantity [5]. The local error is thus potentially influenced by the whole computational domain.

Considering the exact solution ϕ which satisfies the differential operator $\mathcal{L}$ representing the PDE governing this conserved variable, and a grid G_h of size h from which a numerical solution ϕ_h is computed with the ISIS code, then the discretized error is defined as:

$$e_h = \phi - \phi_h$$

An equation for the error is derived by applying the exact operator $\mathcal{L}$ of the PDE that governs ϕ to e_h [6]. For a linear operator the following equation can be derived:

$$\mathcal{L}(e_h) = \mathcal{L}(\phi) - \mathcal{L}(\phi_h) = 0 - \mathcal{L}(\phi_h) = -\mathcal{L}(\phi_h) = S_h$$

From this equation, it can be observed that the error is driven by *the same transport rules* than the solution ϕ itself and the extra source term comes from *the truncation of functions* that appeared in $\mathcal{L}$.

For a nonlinear operator the same analysis is not possible but similar features are expected [7]. Thus, the operator $\mathcal{L}$ of the Navier–Stokes equations is linearized as it was already done [8].

The source term of the resulting equation cannot be computed exactly as it involves the exact operator of the PDE. A higher order discretized operator $\mathcal{L}_h^*$ is considered in order to obtain an approximation S_h^* of S_h. For this approximation to be reliable, $\mathcal{L}_h^*$ must be more accurate than the discretized operator $\mathcal{L}_h$ of the flow solver. The higher order finite-volume discretized operator is obtained by a cubic reconstruction of ϕ_h and its derivatives at nodes and center of faces of the control volume and by integration over faces by the Simpson's rule. The whole discretization is formally fourth order accurate. And, as $\mathcal{L}_h^*$ is fourth order accurate and $\mathcal{L}_h$ is at most second order accurate, a good approximation of this source term is thus expected. It can be noted that as it is an evaluation of the differential residual, the distribution and the magnitude of the source term share no similarity with the error.

Concerning the resolution of the equation for the error, we have shown a posteriori that it is not necessary to use the higher order operator. Both $\mathcal{L}_h^*$ and $\mathcal{L}_h$ have been considered for solving the equation and close results have been obtained for the error field. Consequently, the error can be computed with the same method (and on the same grid) used for solving the PDE of ϕ [6]. Finally, the equation that leads to an estimation of e_h is:

$$\mathcal{L}_h(e_h) = -\mathcal{L}_h^*(\phi_h) = S_h^*$$

More information on the developments of this method and its results can be found in [9].

4. Adaptive techniques

The goal of the adaptive procedure is clearly to reduce the discretization error for reaching a solution of prescribed accuracy for a low computational cost. However, one also wishes to equidistribute the error over the whole computational domain for the solution to be of similar accuracy everywhere. In order to do so, each control volume marked for grid refinement is subdivided into several smaller ones of *the same topology*. As the initial mesh can possibly be too fine in some region for the desired accuracy, it can be coarsened by an *agglomeration algorithm*. The adaptive procedure is completely included in the ISIS code making it an automatic single numerical tool.

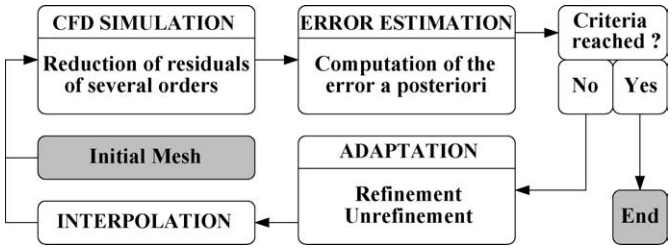

Fig. 1. Adaptive procedure.

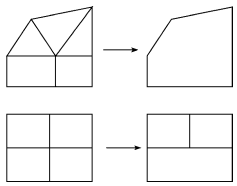

Fig. 2. Agglomerated cells.

4.1. Adaptive procedure

The adaptive procedure is summarized on Fig. 1. It starts with the computation of a first numerical solution on an initial uniform grid with an arbitrary number of cells. The numerical error is then estimated by the method described previously and the information from its source term is used to decide which changes should be made on the current mesh. The criteria of selection of a cell i on the current $Grid_j$ are the following:

Refinement: $Err_{Grid_j}(i) > \mathsf{TolR} * \|Err_{Grid_1}\|_{L_1}$

Unrefinement: $Err_{Grid_j}(i) < \mathsf{TolD} * \|Err_{Grid_1}\|_{L_1}$

The parameters TolR and TolD control the intensity of the procedure during one adaptive step for the refinement and the unrefinement process respectively. The numerical solution is then 'mapped' on the new adapted mesh and the computation is resumed on this grid. This procedure is repeated until the error estimate is below a desired value. In practice a reduction of a factor Red of the L_1 norm of the error over the domain is asked for handling the accuracy of the numerical solution. Thus, the procedure ends when the current $Grid_j$ satisfies:

$$\|Err_{Grid_j}\|_{L_1} < \frac{\|Err_{Grid_1}\|_{L_1}}{\mathsf{Red}}$$

4.2. Grid alteration

During the refinement process, each control volume to be refined is split into several smaller ones of the same topology. The refinement process can occur with a possible directional sensitivity for flows with simple features. A non-refined neighbor of a refined cell presents a so called *hanging node* which is accounted for naturally by our face-based finite-volume method: a face with a hanging node is simply seen as several smaller faces.

The agglomeration algorithm permits to coarse the selected parts of the mesh by grouping neighboring cells marked for unrefinement. The different groups are then merged into a bigger cell. The agglomeration can result from a fusion of a face or of a node as illustrated on Fig. 2.

All these possible grid alterations can be canceled as the initial mesh can be recovered by the use of connectivities between the different generations of meshes. Thus, the regions of the mesh that must be adapted are allowed to change during the computation as it is the case for unsteady computation.

5. Numerical application

5.1. Definition of the problem

The problem consists in simulating the flow of air for a Reynolds number of 22 000 around a square-cross section cylinder located in the vicinity of a solid wall as measured using Laser Doppler Velocimetry by Wu and

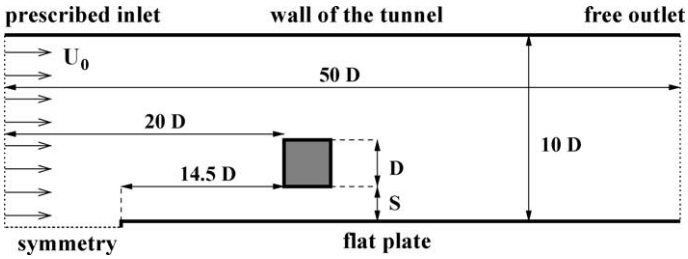

Fig. 3. Computational domain.

Martinuzzi [10]. The experimental geometry is described on Fig. 3. With a gap between the plate and the bottom square-cross section cylinder of $S/D = 0.25$, the flow is stationary.

The RANS equation are considered for simulating this turbulent flow. The closure of the equations is done by the two-equation k–ω turbulence model of Menter [2] which is a good compromise between computational effort and an accurate physical modelling. Details on the computational domain and boundary conditions can be found in [11].

For this nonlinear problem, the exact solution is not known. In order to evaluate the quality of the adapted solutions, a uniform grid refinement study has been performed. Six uniform grids of increasing fineness have been considered for making single mesh computations. Their numbers of cells range from 4288 up to 550 000 for the uniform Grid 6 (see Table 1). The different solutions obtained from the considered grids converge to a practically mesh independent solution which will be used as a reference for evaluating the quality of the adapted solution.

5.2. Results

Any of the uniform grids can be used as the initial grid of the adaptive procedure since this initial mesh can be refined but also coarsened if it appears too fine in some regions for the desired accuracy. However, the coarser the first grid is and the less time consuming the adaptive computation is. Thus, the coarsest uniform mesh (Grid 1) is used as the starting point of the present computation.

The norm of the error vector of the velocity, defined by $Err(\|\vec{U}\|) = \sqrt{Err(U)^2 + Err(V)^2}$, and the error for the kinetic turbulent energy k were considered in the adaptive process. The turbulence model plays an important role on all the variables that are to be solved in this problem and therefore the accuracy of its resolution influences the quality of the whole solution. It is believed a priori that taking into account the error for k allows one to resolve accurately the turbulent properties of the flow since the kinetic turbulent energy is linked to the intensity of turbulence. Consequently, three additional equations have to be solved at each adaptive step (one for each velocity component and one for k). Fortunately, these equations are linear (see Section 3) so that the computational overhead for solving them is negligible.

The parameters that control the adaptive procedure are $\mathsf{TolR} = 0.4$, $\mathsf{TolD} = 0.08$ and $\mathsf{Red} = 5$. The same tolerance of refinement TolR is applied for the treatment of $\vec{U}$ and k. For reaching the chosen criterion of reduction of the L_1 norm of the errors considered, three adaptive steps of isotropic refinement were performed and the resulting final adapted mesh has 35 314 computational points. The initial uniform mesh and the final adapted mesh obtained after the three cycles of adaptation are presented in Fig. 4. The regions that were refined or coarsened can clearly be seen along with the agglomerated cells created by unrefinement of the initial mesh. The unrefinement process was not intense since the starting grid is already coarse. A closer view around the square cylinder of the different meshes generated during the adaptive procedure is also presented in Fig. 5 with the corresponding error fields of $\vec{U}$ normalized by the L_1 norm of its quantity on the initial mesh ($\|Err_{Grid_1}(\vec{U})\|_{L_1}$). The evolution of these estimated error fields shows that the goal of this adaptive procedure is achieved as the error is both reduced and equidistributed over the whole computational domain. It also can be seen that the adaptive procedure converges

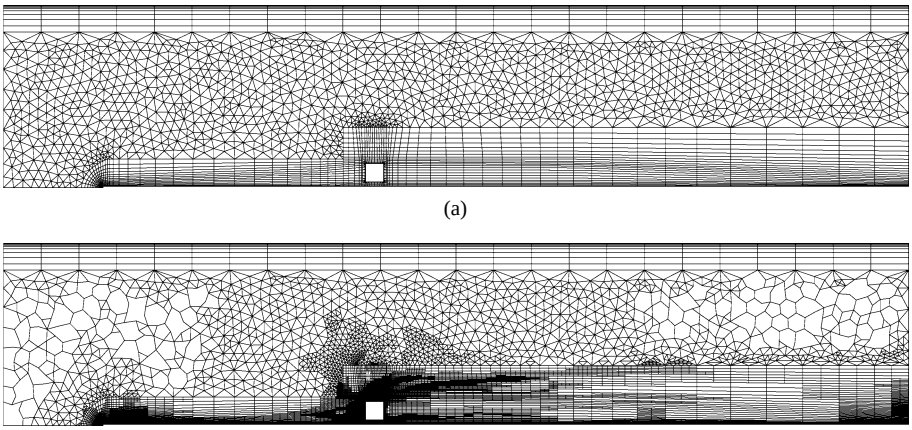

(a)

(b)

Fig. 4. Global view of the meshes. (a) Initial uniform mesh (4288 cells), (b) final adapted mesh (35 314 cells – 3 adaptive steps).

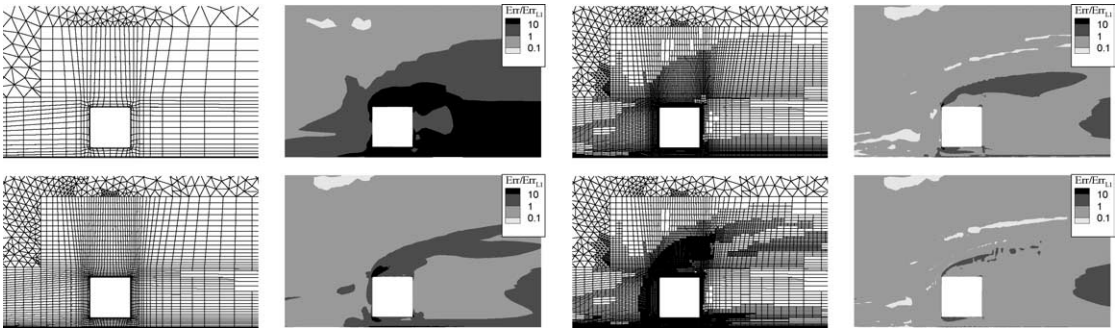

Fig. 5. Inside view of the adapted procedure near the square cylinder.

Table 1
Informations on computations

	Nb of cells	CPU time
Grid 1	4288	1
Grid 2	8355	3.27
Grid 3	16 733	13.89
Grid 4	68 293	138.06
Grid 5	135 436	709.65
Grid 6	550 609	7162.86
Adaptive	35 314	69.77

Table 2
Computed recirculation length

	L_{rec}	$Err_{\text{rel}}(L_{\text{rec}})$ (%)
Grid 1	5.9385	14.5
Grid 2	5.6576	9.1
Grid 3	5.9208	14.1
Grid 4	5.4766	5.6
Grid 5	5.3428	3.0
Grid 6	5.1872	–
Adaptive	5.1734	0.3

since the refined areas are smaller and smaller during the adaptive procedure. Fig. 6 presents the streamlines around the square-cross section cylinder for the velocity fields computed on the initial uniform grid, the final adapted grid and the finest uniform grid respectively. It can be observed that the adapted grid velocity field is in close agreement with the reference finest grid solution. The small recirculation located below the bottom face of the square cylinder is not captured on the coarse uniform grid but well simulated on the adapted grid. Fig. 7 presents a comparison of the profiles of the normalized streamwise component of the mean flow U/U_∞, for the all the grids considered, extracted at $X/D = 0$, i.e. on the middle top face of the square cylinder. The profiles of the normalized shear component of the Reynolds stress are also given. Firstly, one can remark that the uniform grids effectively converge

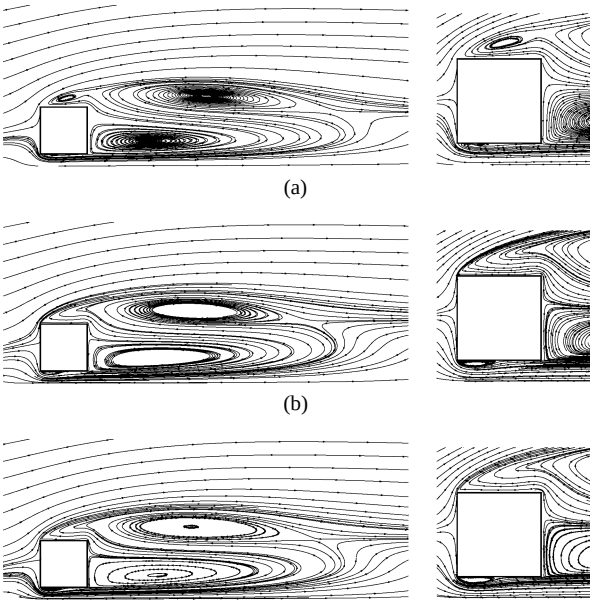

(a)

(b)

(c)

Fig. 6. Streamlines around the square cylinder. (a) Uniform Grid 1, (b) final adapted grid, (c) Uniform Grid 6.

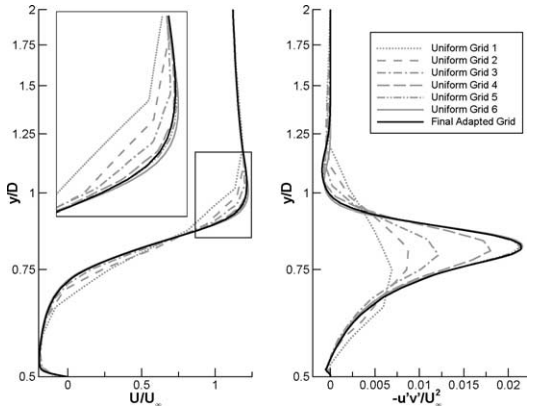

Fig. 7. Profiles extracted at $X/D = 0$.

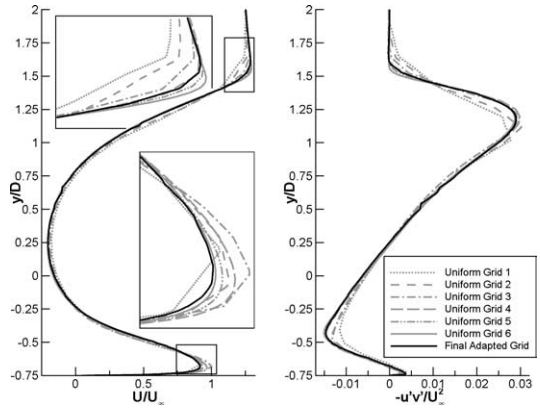

Fig. 8. Profiles extracted at $X/D = 2$.

to a practically mesh independent solution as announced in the previous section. Secondly, it can be concluded from these profiles that the solution of the adaptive procedure has reached the fine grid solution. This is especially true for the turbulent correlation. More precisely, the adapted solution profiles are close to the ones obtained on the uniform Grid 5 so that the two computations can be considered as comparable in terms of accuracy. In Fig. 8, the same profiles are extracted at $X/D = 2$, i.e. in the wake of the square cylinder. Once again, these profiles indicate that the solution of the adaptive computation is comparable to the uniform Grid 5 solution.

Finally, Table 2 gives the recirculation length along the plane $y = 0$ for the different uniform meshes used in the grid refinement study and for the final adapted meshes. It can be seen from the values of the relative errors ($Err_{\text{rel}}(L_{\text{rec}})$) with respect to the finest uniform grid (Grid 6) that the recirculation length computed by the adaptive procedure is very good since it is located between the ones of Grid 5 and Grid 6. From all these results, it can

be concluded that the adapted grid solution is at least of comparable accuracy to the one of the uniform Grid 5 solution.

In order to quantify the gains obtained by the use of the adaptive procedure compared to single uniform mesh computation, Table 1 presents also the number of computational points of the different meshes considered in this study and the CPU time (relative to the one of the coarsest uniform grid) needed for reaching a converged solution. The CPU time for the adaptive computation referred to the whole adaptive procedure from the initial grid to the final adapted grid including error estimations. Compared to the uniform Grid 5, which has been demonstrated of the same accuracy, the adaptive computation requires almost 4 times less computational points and more than 10 times less CPU time.

6. Conclusions

An error estimate designed in the framework of finite-volume methods and based on an equation for the discretization error has been presented. An adaptive h-refinement procedure guided by the normalized source term considered in the error estimate has also been described. It has been shown to be general since the initial mesh can be both refined and coarsened. The adaptive procedure included in the ISIS flow solver is a complete automatic single tool for reaching solutions with a desired accuracy for a low computational cost. This tool has shown interesting gains for a complex two-dimensional turbulent flow in term of CPU time and memory requirement compared to single mesh computations.

References

[1] P.R. Spalart, S.R. Allmaras, A one-equation turbulence model for aerodynamic flows, AIAA 30th Aerospace Sciences Meeting, AIAA Paper 92-0439, Reno, NV, 1992.
[2] F.R. Menter, Zonal two-equation k–ω turbulence models for aerodynamic flows, AIAA 24th Fluid Dynamics Conference, AIAA Paper 93-2906, Orlando, FL, 1993.
[3] G.B. Deng, M. Visonneau, Comparison of explicit algebraic stress models and second-order turbulence closures for steady flow around ships, in: 7th Symposium on Numerical Ship Hydrodynamics, Nantes, France, 1999, pp. 1–15.
[4] P.J. Roache, Quantification of uncertainty in computational fluid dynamics, Annu. Rev. Fluid Mech. 29 (1997) 123–169.
[5] R. Rannacher, Error Control and Adaptivity in Scientific Computing, Kluwer Academic, 1999, pp. 247–278.
[6] I. Celik, G. Hu, Discretization error estimation using error transport equation, in: ASME 2002 Fluids Engineering Division Summer Meeting, July 14–18, Montreal, Quebec, Canada, 2002.
[7] J.H. Ferziger, M. Perić, Computational Methods for Fluid Dynamics, third ed., Springer-Verlag, Berlin, 2002.
[8] X.D. Zhang, J.-Y. Trépanier, R. Camarero, A posteriori error estimation for finite-volume solutions of hyperbolic conservation laws, Comput. Methods Appl. Mech. Engrg. 185 (2000) 1–19.
[9] A. Hay, M. Visonneau, Adaptive error control strategy: application to a turbulent flow, AIAA 16th Computational Fluid Dynamics Conference, AIAA Paper 2003-3848, June 23–26, Orlando, FL, 2003.
[10] K.C.Q. Wu, R.J. Martinuzzi, Experimental study of the turbulent wake flow behind a square cylinder near a wall, in: ASME Fluids Engineering Division Summer Meeting, Canada, Vancouver, 1997, pp. 1–7.
[11] E. Guilmineau, P. Queutey, Numerical study of the turbulent flow around a square cylinder near a wall, in: International Mechanical Engineering Congress and Exhibition, IMECE 2002-32285, November 17–22, New Orleans, LA, USA, 2002.